20th International Conference on Structural Mechanics in Reactor Technology (SMiRT 20)
Espoo, Finland, August 9-14, 2009
SMiRT 20-Division ??, Paper ??

Simulation of roll expansion on Steam Generator tubes

MESSIER Julien[1], CANO Valérie[1], GENIAUT Samuel[1], HASNAOUI Frédéric[2], SELLALI Nabila[1]

[1]EDF R&D, 1 avenue du Général de Gaulle, B.P. 408 , F-92141 Clamart Cedex
[2]EDF R&D, 6 quai Watier, B.P. 49, F-78401 Chatou Cedex

Keywords: Steam Generator, Code_Aster, roll expansion, cracks, tubes, contact.

1 ABSTRACT

In order to understand and predict crack phenomena aiming to obtain safety margin assessment, we need to evaluate, by numerical simulation, the residual stress field due to the roll expansion of the steam generator fabrication process.
The whole process has been idealized with Code_Aster, Open Source FEA software developed at EDF R&D, through a 3D model integrating contact and an elastic-plastic behaviour identified from experimental tests.
The quality of the obtained results is evaluated through a comparison with previous experimental and numerical works. This simulation leads to a fine description of the residual stress field and brings a significant improvement to estimate the contribution of the fabrication process on crack formation in PWR operating conditions, as well as crack behaviour in primary circuit hydraulic pressure test conditions.

2 INTRODUCTION

Steam Generators tubes constitute critical PWR components owing to their heat exchange function as well as their function of safety barrier between primary and secondary circuits.

Among the current Steam Generator tubes, many crack networks can be observed in the transition roll expansion area. These cracks can have many causes, but they are essentially linked with:

- fabrication process (residual stresses due to mechanical roll expansion),
- operating loads (thermal and hydraulic cyclic solicitations, primary and secondary corrosion).

In order to understand these phenomena aiming to obtain safety margin assessment, and eventually be able to optimise the fabrication process, we need to evaluate, by numerical simulation, the residual stress field due to the roll expansion.
Indeed, a thorough knowledge of these stress fields is necessary in order to understand and predict crack phenomena.

This study is carried on with the most common material of the French steam generator : the Inconel 600. The kind of the involved expansion is composed by a principal one that will be named “Integral Expansion” (IE) located on the whole depth of the tube sheet, and a second one named “mechanically ameliorated” (MAE) which is smaller than the previous one and is located above the tube sheet (Fig. 1). This configuration is the one leading to the biggest number of cracks.

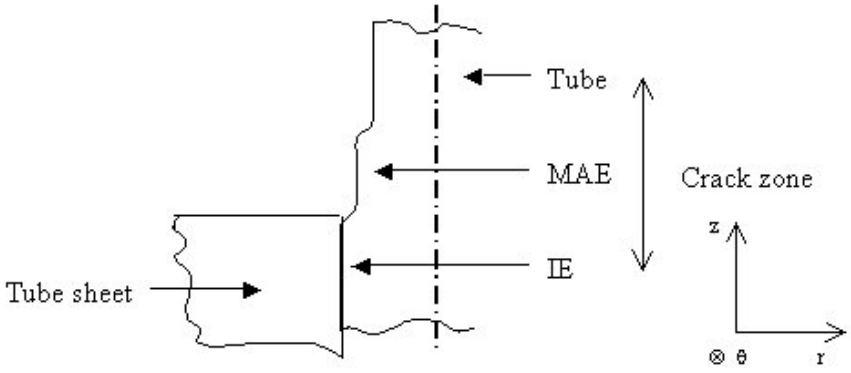

Figure 1. : Schematic representation of expansion variation zone of a Steam Generator tube

With computing material, geometrical and operating data, a numerical model can be built in order to faithfully reproduce the fabrication process and its structural consequences in term of residual stress field.
This model and its results can then respectively be used on further simulations such as fracture mechanics and hydromechanics in order to estimate a flow rate through the crack.

3 METHOD

In the early 90's, experimental and theoretical works gave a good evaluation of the residual stress field on the inner surface of the tube in its main directions.
Nevertheless, the great improvements of calculation means allow us today to make this result more complete and, particularly, to obtain a full evaluation of the stress field in the whole structure through a realistic representation of contact between the tool and the tube.

Code_Aster[1] , Open Source FEA software developed at EDF R&D, is appropriate to solve non-linear mechanical analyses, such as roll expansion simulation that combines non-linearities from contact and from the material behaviour.
We validate our model and our hypotheses, on the one hand, by satisfying the fabrication tolerances and, on the other hand, by fitting the results of previous works.

To this end, we proceed in several steps of validation using models with growing complexity:

- 2D-Axi-symmetric,
- 2D in a radial-transverse section, allowing to specifically study the effects of the tool rotation,
- 3D with radial load in order to reproduce in 3D the 2D-Axi-symmetric results,
- 3D with the complete tool realistic rotational motion. The great supply of this 3D model is to be able to catch the effects of the tool displacement in terms of eventual stress singularities on every point of the structure and thus, to predict their consequences in presence of cracks.

3.1 Hypotheses

3.1.1 Material behaviour

- ***Tube***

In order to faithfully idealize the tube material behaviour, different experimental tests have been realized : pure tensile tests and compression/tensile cyclic tests.
A first step was to select a law able to reproduce the both kinds of tests. In other words, this law should have to fit first and stabilized cycles as well as assess a numerical convergence of calculation. This goal could not be achieved with a Chaboche law.
We decided to simplify the identification by separately considering elastic and plastic slope (Fig. 2) and implementing a Von Mises behaviour law with a combined work-hardening including both linear kinematic and isotropic parts.
We verified afterwards the acceptable fitting of this law with the experimental cyclic test responses (Fig. 3).

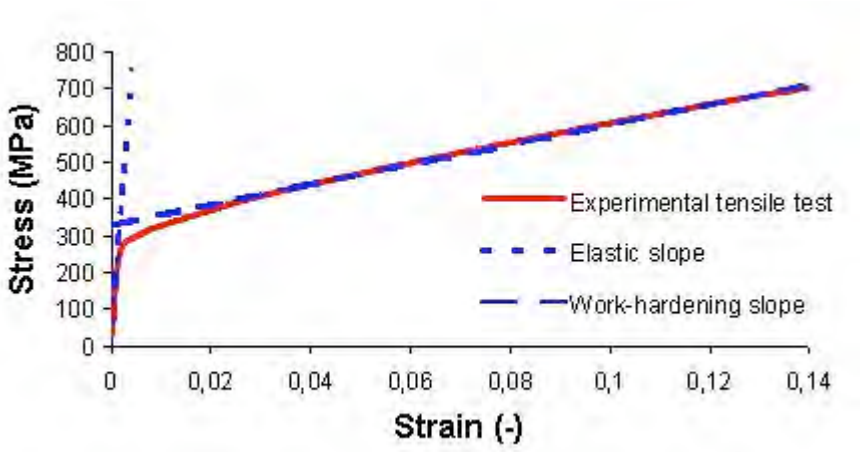

Figure 2. Identification of the elastic-plastic behaviour of the tube

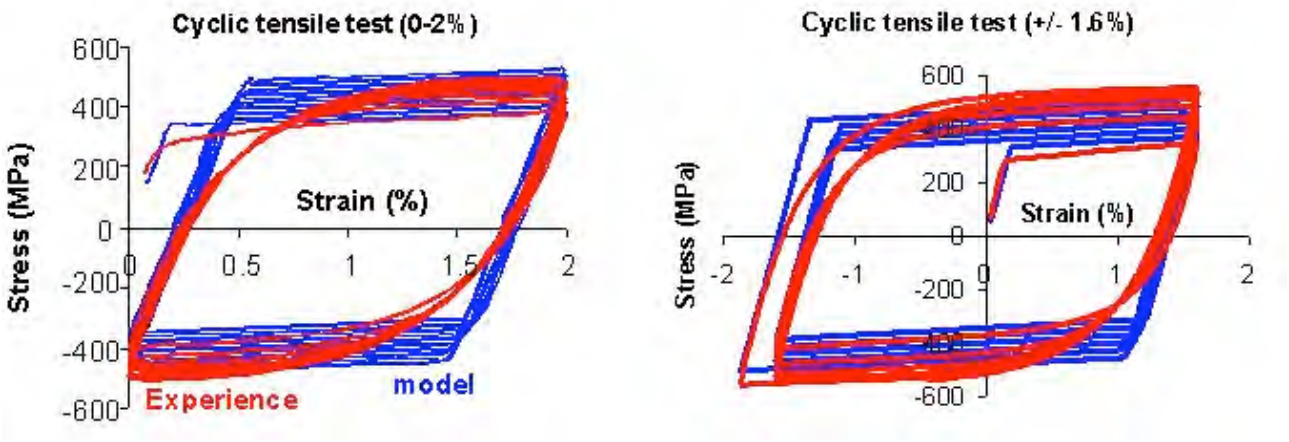

Figure 3. Identification of the cyclic behaviour of the tube

- ***Tube sheet***

The tube sheet is made of 16MND5 steel. Two different zones are considered :

- **Zone 1**, close to the tube, where the behaviour of the tube sheet is considered elastic-plastic with isotropic work-hardening,
- **Zone 2,** far from the tube, where the behaviour of the tube sheet is considered linear elastic and the transverse orthotropy is homogenized into transverse isotropy.

- ***Rolling tool***

We are not interested in the eventual deformation of the tool during the process. We consider it keeps its shape and so, we do not affect any mechanical behaviour to the tool.

3.1.2 Mesh and geometry

We decided to idealize rolling tool, tube-sheet and tube in a restrictive zone where cracks can occur: the expansion transition zone. Considering the bending wave absorption in the both directions from the tool head, this zone begins 10 mm under the upper part of the tube-sheet to end 60 mm above it.

The meshes of the different models are made in gibiane language, using quadrangular face elements. Different shape functions have been tested (linear and quadratic). The sensibility of the results to the order of these functions showed the necessity to use quadratic elements: oscillations being found with refinement by using linear elements.

The corresponding meshes of two different models that have been used are represented on Fig.4 and Fig.5.

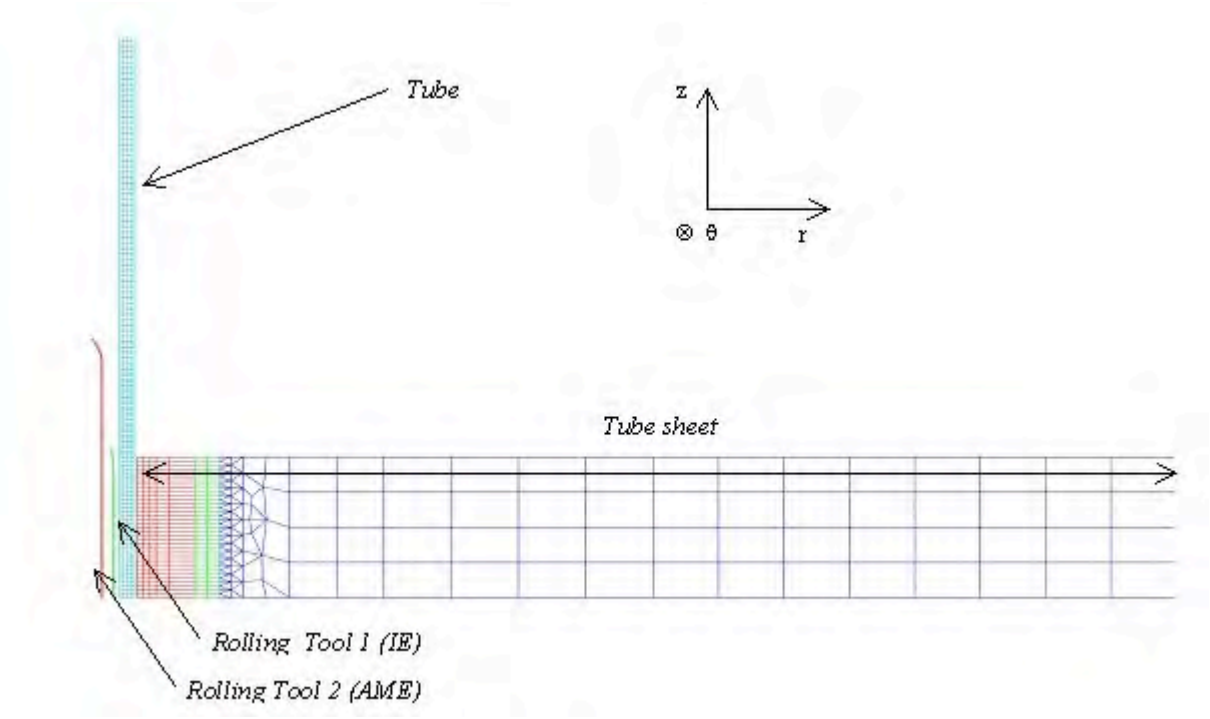

Figure 4. 2D-Axi-symmetric model

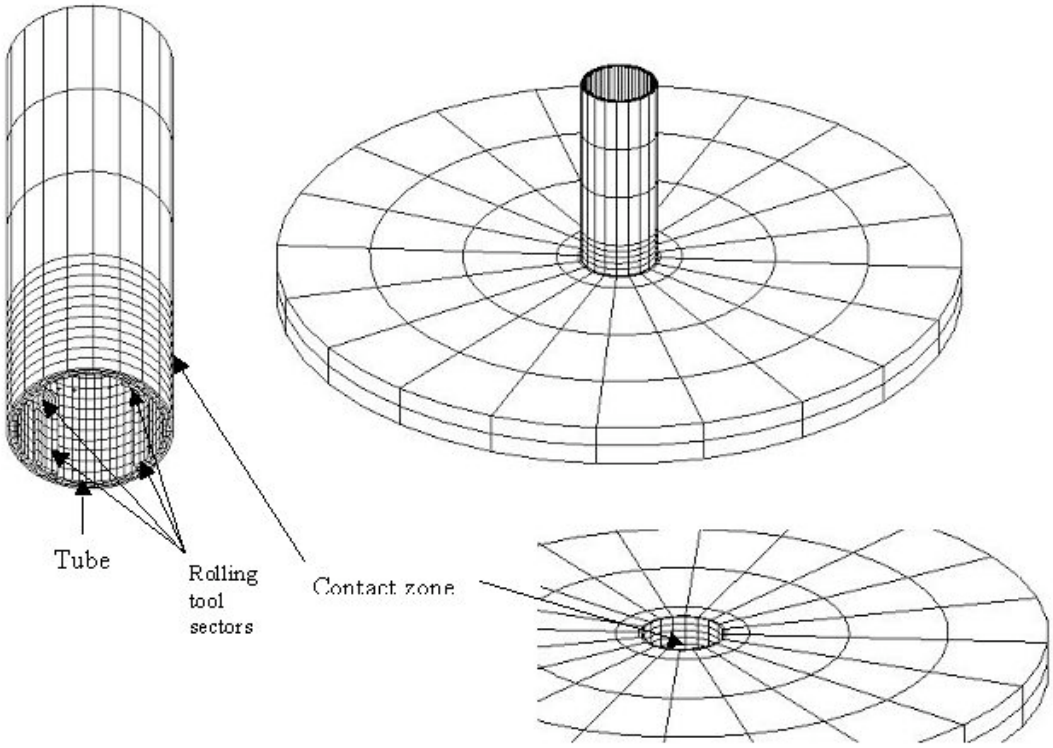

Figure 5. Full 3D model

3.1.3 Boundary conditions and applied load

- **Contact**

Contact surfaces are defined on the one hand between rolling tool and tube, and on the other hand, between tube and tube-sheet. We do not define any friction coefficient, assuming contact remains normal and punctual between the tool and the tube during the load - which is true when the tool rolls without sliding inside the tube. Besides, we assume the only existence of radial motion between tube and tube sheet, which allows us to ignore any eventual friction between these two elements.

- **Blocked displacements**

Representing the fastening of the neighbor structure, the displacement of the bottom surface of all the components is blocked in its normal direction so the side face of the tube sheet.
Representing the fastening of the tube at the top of the Steam Generator, the displacement of the upper surface of the tube is blocked in the 3 directions.

- **Prescribed displacements**

The mechanical load is only due to the prescribed displacement of the tool in contact with the tube.
In the full-3D model, we decide to decompose the process in three steps.

- 1 : the tool revolution is a spiral inside the tube,
- 2 : the tool revolution is a circle inside the tube with the same radius as the position reached at the end of the spiral,
- 3 : the tool is instantly unloaded at the end of the circle.

Table 1. Description of the spiral rolling tool displacement

Pos.	Initial instant	Disp.	Inst$_i$	Inst$_i$ = 2πN
X_Gj	$\sqrt{x_0^2+y_0^2}\left(\cos\left(\arctan\left(\frac{y_0}{x_0}\right)\right)\right)$	DX_Gj	$\sqrt{x_0^2+y_0^2}\left(\cos\left(Inst_i+\arctan\left(\frac{y_0}{x_0}\right)\right)-\cos\left(\arctan\left(\frac{y_0}{x_0}\right)\right)\right)+\frac{Inst_i}{2\pi\cdot N}D_{fin}\cdot\cos\left(Inst_i+\frac{(j-1)2\pi}{n}\right)$	$D_{fin}\cdot\cos\left(\frac{(j-1)2\pi}{n}\right)$
Y_Gj	$\sqrt{x_0^2+y_0^2}\left(\sin\left(\arctan\left(\frac{y_0}{x_0}\right)\right)\right)$	DY_Gj	$\sqrt{x_0^2+y_0^2}\left(\sin\left(Inst_i+\arctan\left(\frac{y_0}{x_0}\right)\right)-\sin\left(\arctan\left(\frac{y_0}{x_0}\right)\right)\right)+\frac{Inst_i}{2\pi\cdot N}D_{fin}\cdot\sin\left(Inst_i+\frac{(j-1)2\pi}{n}\right)$	$D_{fin}\cdot\sin\left(\frac{(j-1)2\pi}{n}\right)$

Where **inst** is the calculation step, $\mathbf{x_0}$ and $\mathbf{y_0}$ are the initial position of the tool nodes, $\mathbf{D_{fin}}$ the final radial expansion, **j** the number of the tool, **n** the total number of tools and **N** the number of laps to do (N=1).

Table 2. Description of the circular rolling tool displacement

Pos.	Initial instant	Disp.	Inst$_i$
X_Gj	$\sqrt{x_1^2+y_1^2}\cdot\left(\cos\left(\arctan\left(\frac{y_1}{x_1}\right)\right)\right)$	DX_Gj	$\sqrt{x_i^2+y_i^2}\cdot\left(\cos\left(Inst_i+\arctan\left(\frac{y_i}{x_i}\right)\right)-\cos\left(\arctan\left(\frac{y_i}{x_i}\right)\right)\right)+D_{fin}\cdot\cos\left(\frac{(j-1)2\pi}{n}\right)$
Y_Gj	$\sqrt{x_1^2+y_1^2}\cdot\left(\sin\left(\arctan\left(\frac{y_1}{x_1}\right)\right)\right)$	DY_Gj	$\sqrt{x_i^2+y_i^2}\cdot\left(\sin\left(Inst_i+\arctan\left(\frac{y_i}{x_i}\right)\right)-\sin\left(\arctan\left(\frac{y_i}{x_i}\right)\right)\right)+D_{fin}\cdot\sin\left(\frac{(j-1)2\pi}{n}\right)$

where $\begin{cases} x_1 = x_0 + D_{fin}\cdot\cos\left(\frac{(j-1)2\pi}{n}\right) \\ y_1 = y_0 + D_{fin}\cdot\sin\left(\frac{(j-1)2\pi}{n}\right) \end{cases}$

The maximal tool displacement is adjusted to satisfy fabrication criterion: tube thickness should present a thinning rate $\boldsymbol{\tau_s}$ around 4 % at the end of the process. That allows us to determine analytically, with a sufficient approximation, the value of he parameter $\mathbf{D_{fin}}$ for the primary expansion.
By respectively noting $\mathbf{R_{int}}$ and $\mathbf{R_p}$ the initial inner radius of the tube and tube-sheet, and **e** the initial tube thickness, we can write:

$$D_{fin}=R_p-R_{int}-e(1+\tau_s)$$

With similar considerations, by noting $\mathbf{R_{ext}}$ the initial outer radius of the tube and $\boldsymbol{\Delta_{MAE}}$ the final wanted displacement for the tube in the secondary expansion, we can write:

$$D_{fin}=\sqrt{(R_{ext}+\Delta_{MAE})^2-R_{ext}^2+R_{int}^2}-R_{int}$$

4 RESULTS

4.1 Model validation

The different models are validated through the quality of the obtained results in terms of displacements, thinning and stress after unload of the structure.
These results are taken on a longitudinal line of the inner and outer skin of the tube.

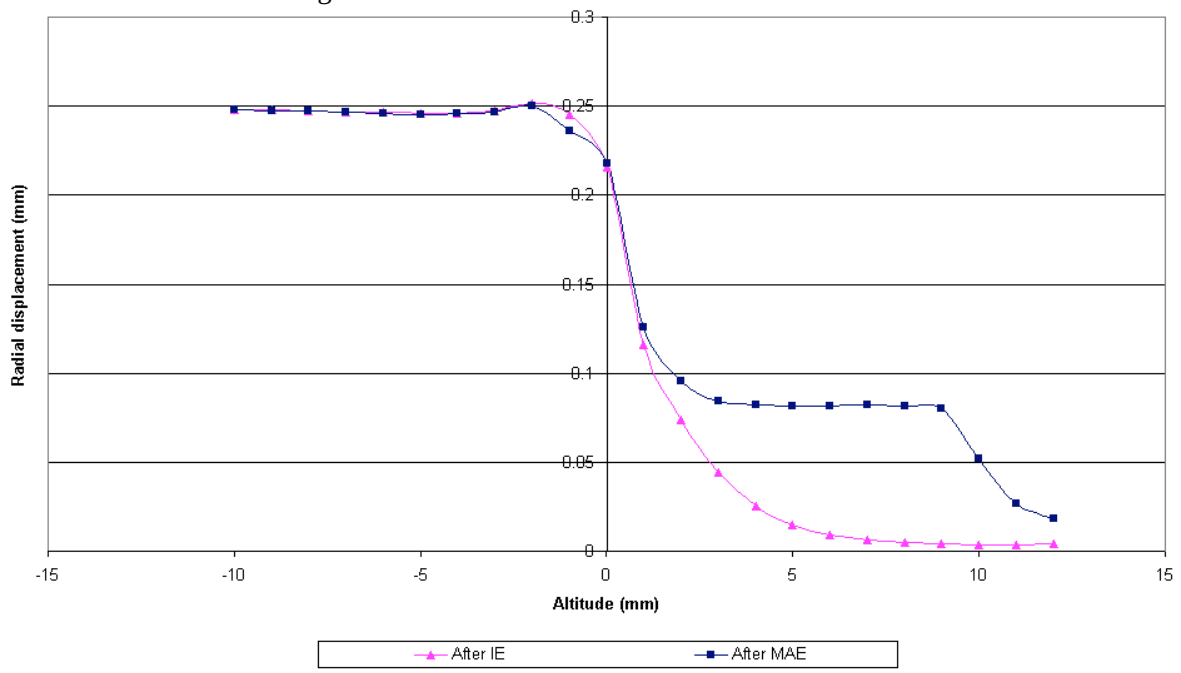

Figure 6. Inner skin profile after unload with Full-3D model

The Fig.6 shows that contact does not bring any perturbation on the structure profile where the only prescribed displacement clearly appears.

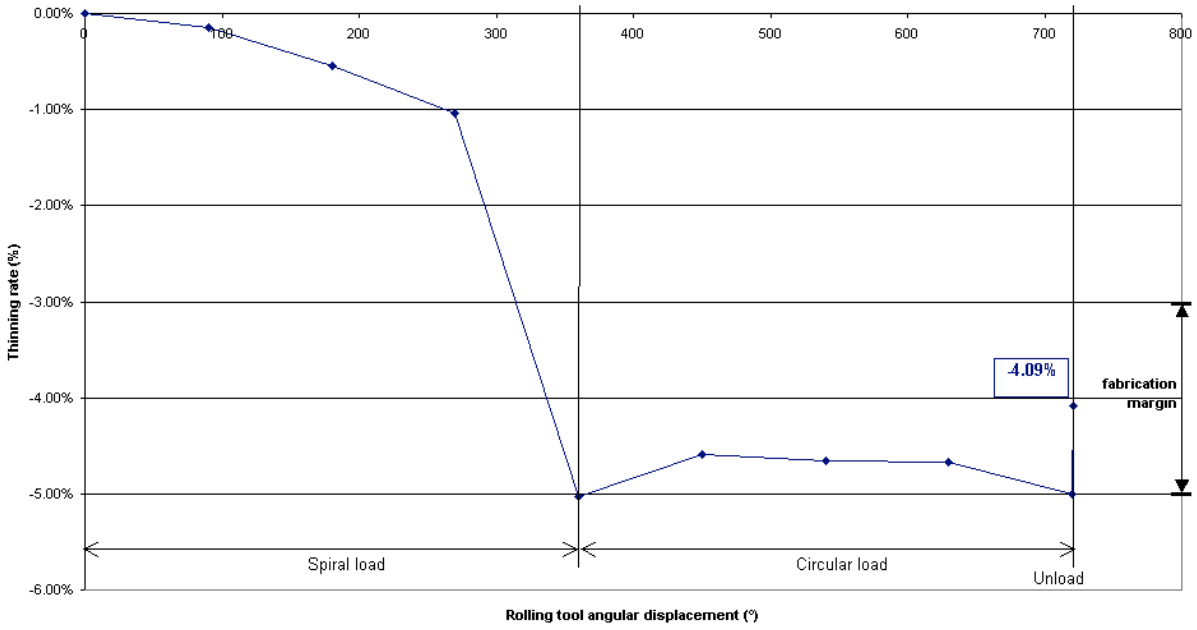

Figure 7. Thinning rate evolution with Full-3D model

The Fig.7 shows that the final thinning rate of the tube after unload is very acceptable with respect to fabrication margin.

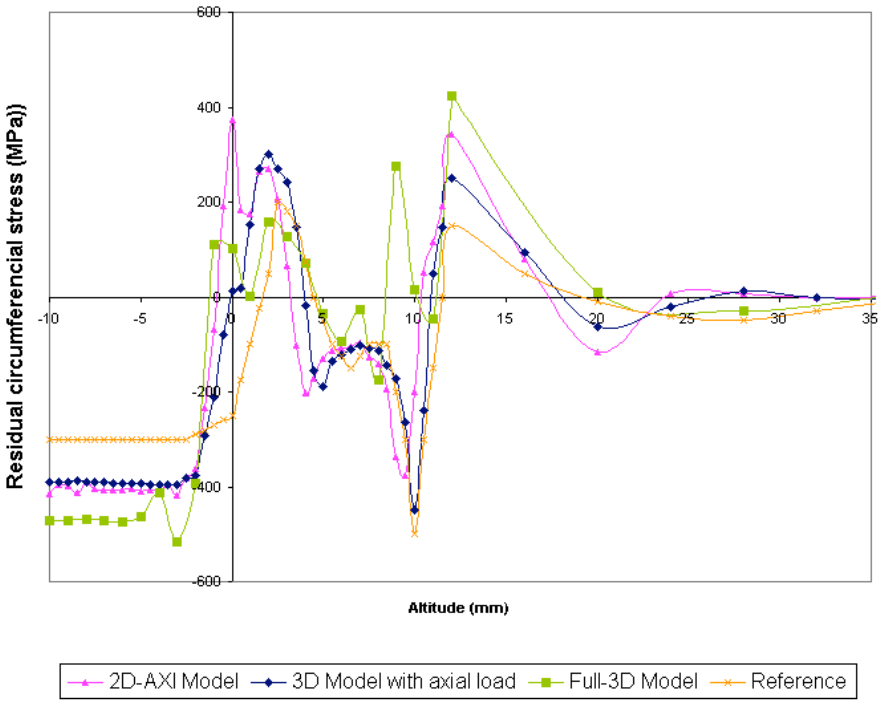

Figure 8. Comparison of the residual stress on the inner skin of tube for the different models

The Fig.8 shows a good fitting between the three different models, one with each other and also with the global shape of the reference curve.

The higher stress level obtained with the full-3D is certainly involved with tool contact. Indeed, geometry can create stress singularities such as those appearing in the neighbourhood of the head of the MAE rolling tool (z ≈10mm).

4.2 3D contribution

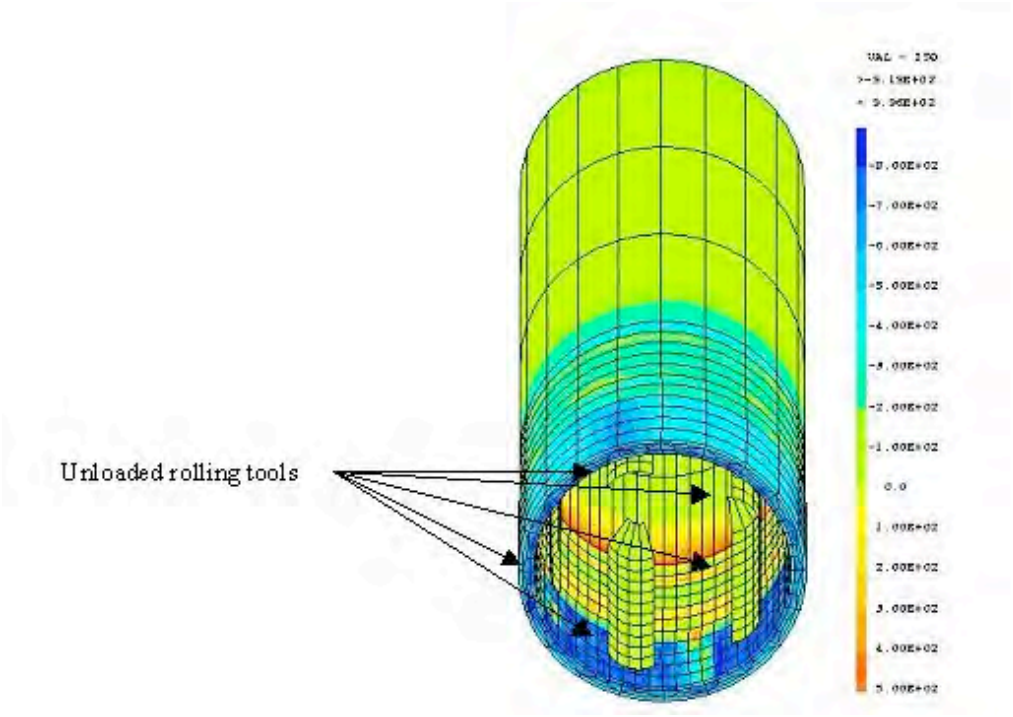

Figure 9. Projection of the circumferential residual stress field on the deformed mesh after unload

By solving the mechanical problem all along the tool displacement, we can access to the strain and stress on every integration point of the structure during the load.

On the Fig.9 representing the circumferential stress field on the unloaded structure, we can distinguish the bottom zone where the tube has been compressed between tool and tube-sheet, and a upper zone where the inner skin of the tube has been stretched under the MAE rolling tool. Thus, a good knowledge of the circumference stress field allows us to locate before any other calculation, where an eventual longitudinal crack would open mostly in Mode I.

We can point stress singularities in the tube circumference and link them with the unload of the rolling tool. Indeed, the yielding due to this instantly unload creates a calking of the inner skin. This particularity would have been prevented with a slower unload.

This obtained residual stress field can, for instance, be stored and directly projected on a cracked structure in order to estimate the contribution of the fabrication process on crack opening for different configurations of cracks.

5 CONCLUSION

The identification and implementation of the tube material behaviour from experimental tests were the necessary condition to build a mechanical model in order to simulate the roll expansion.

Justifying hypotheses on contact, displacement and boundary conditions, a full-3D model could have been validated through a comparison with simpler models and previous experimental works.

By leading to a fine description of the residual stress field, it brings a significant improvement to estimate the contribution of the fabrication process on crack formation in PWR operating conditions, as well as crack behaviour in primary circuit hydraulic pressure test conditions.

[1] www.code-aster.org